

9.21 Single Molecule Fluorescence Methods in Enzymology

Peng Chen and Nesha May Andoy, Cornell University, Ithaca, NY, USA

© 2010 Elsevier Ltd. All rights reserved.

9.21.1	Introduction	751
9.21.2	Fluorescent Active Site	752
9.21.2.1	Principle	752
9.21.2.2	Example: Catalytic Dynamics of Cholesterol Oxidase	753
9.21.2.3	Features and Generality	753
9.21.2.4	Challenges	753
9.21.3	Fluorogenic Reaction	755
9.21.3.1	Principle	755
9.21.3.2	Example 1: β -Galactosidase with Single-Turnover Detection	755
9.21.3.3	Example 2: β -Galactosidase with Microchamber Encapsulation	757
9.21.3.4	Features and Generality	757
9.21.3.5	Challenges	757
9.21.4	Fluorescent Substrate	758
9.21.4.1	Principle	758
9.21.4.2	Features and Generality	759
9.21.4.3	Challenges	760
9.21.5	Fluorescence Resonance Energy Transfer (FRET)	760
9.21.5.1	Principle	760
9.21.5.2	Example: Conformational Dynamics-Coupled Catalysis of T4 Lysozyme	760
9.21.5.3	Features and Generality	761
9.21.5.4	Challenges	761
9.21.6	Fluorescence Quenching via Energy Transfer	762
9.21.6.1	Principle	762
9.21.6.2	Example: Catalysis of Nitrite Reductase	762
9.21.6.3	Features and Generality	763
9.21.6.4	Challenges	764
9.21.7	Fluorescence Quenching via Electron Transfer	764
9.21.7.1	Principle	764
9.21.7.2	Example: Conformational Dynamics of Flavin Reductase	764
9.21.7.3	Features and Generality	764
9.21.7.4	Challenges	765
9.21.8	Summary	766
References		766

9.21.1 Introduction

The rapid advances in single-molecule methods have enabled many innovative studies in the life sciences. These single-molecule measurements have unraveled the detailed workings of many macromolecular machineries,¹ that would otherwise be hidden in measuring the average behaviors of a population of molecules. Breakthrough discoveries continue to emerge in areas such as molecular motors,^{2–6} protein–DNA interactions,^{7–9} RNA activities,^{10–14} protein folding and dynamics,^{15–19} enzymology,^{20–25} and gene expression.^{26–28}

The power of the single-molecule approach stems from its many distinctive features. First, it removes population averaging so that heterogeneous behaviors of biomolecules can be revealed and subpopulations analyzed. This is particularly important for biological system since heterogeneity easily arises in biomacromolecules, for example, proteins in different conformational states. Second, it removes the need for

synchronization of molecular actions for studying time-dependent processes, as it monitors one molecule at a time. This feature also allows us to visualize the actions of individual biomolecules in real time, which is particularly useful in capturing reactive intermediates and elucidating the mechanisms of biochemical reactions.

Experimental methods to investigate single biomolecules fall into three categories: optical (e.g., fluorescence and nonlinear optical microscopy), mechanical (e.g., optical tweezers, magnetic tweezers, scanning probe microscopy, and microfluidics), and electrical measurements (e.g., patch clamp and nanopores). All these methods allow real-time observation of dynamic processes of individual biomolecules. Among these methods, single-molecule fluorescence techniques are perhaps one of the most popular because of their straightforward instrumentation and easy operation.^{4,29–32} One can monitor the fluorescence intensity, spectrum, polarization, or lifetime of a biomolecule to investigate its molecular properties; among these, following fluorescence intensities is the most straightforward. Introducing exogenous fluorescent labels is a general strategy when the target biomolecules are not naturally fluorescent.

To achieve single-molecule fluorescence detection, there are three common experimental practices. First, experiments are done at low concentrations (10^{-9} – 10^{-12} mol l⁻¹) to spatially separate molecules, so each of them can be studied without interference from surrounding molecules. Second, fluorescence signal detection is confined to a small volume ($<10^{-15}$ l) to minimize background noises for single-molecule sensitivity. Third, biomolecules are often immobilized, so a single molecule can be studied over time.

Two experimental setups are widely used for single-molecule fluorescence detection: total internal reflection (TIR) fluorescence microscopy and confocal fluorescence microscopy. The evanescent field from TIR confines the laser excitation to a thin layer (~ 50 – 300 nm), whereas the confocal scheme focuses on the laser beam to a diffraction limited volume and uses a pinhole to confine the signal detection around the focus ($\sim 300 \times 300 \times 600$ nm³). The TIR fluorescence microscopy typically uses electron-multiplying cameras as detectors and can image hundreds of molecules simultaneously; the time resolution is about milliseconds limited by the camera speed, although submillisecond imaging is possible with the state-of-the-art hardware and exceptionally bright probes.³³ The confocal microscopy uses point detectors, such as single-photon avalanche photodiodes, and examines one molecule at a time; the time resolution can be up to microseconds for following dynamic processes of biomolecules. For both TIR and confocal microscopy, multiple detection channels, such as different colors and polarizations, can be readily implemented. The laboratory manual edited by Selvin and Ha³⁴ provides a comprehensive account of the technical and application aspects of single-molecule techniques. Many reviews on the principles and applications of these single-molecule methods are also available.^{1,4,5,13,18,28–32,35–53}

The scope of this chapter is limited to single-molecule studies of enzymology, in particular using single-molecule fluorescence techniques. A continuing challenge in structure–function studies of enzymes is to understand the contribution of conformational dynamics to enzyme function. Single-molecule enzymology, with its ability to monitor enzyme reactions in real time at the single-molecule level, can gain insight into how slow conformational dynamics of enzymes are coupled to catalysis.^{12,20–25,54–62}

This chapter is organized as follows: We divide the single-molecule enzymology studies according to their approaches; for each approach, we focus on the principle, features and generality, and experimental challenges, and use examples in the recent literature for illustrations. For different perspectives on single-molecule enzymology studies, we refer the readers to previous reviews,^{47–50,62} in particular the extensive review by Hammes and coworkers.⁴⁸ We also want to point out that some content of this chapter overlaps with a recent review article by the authors on single-molecule studies of biological inorganic systems.⁵⁰

9.21.2 Fluorescent Active Site

9.21.2.1 Principle

Many enzymes use organic cofactors, such as flavin and porphyrin, at the active sites for catalysis. Some of these organic cofactors, especially flavin, have intrinsic fluorescence, and can be imaged readily at the single-molecule level. If the fluorescence of these cofactors is coupled with the state of the active site in the catalytic cycle, monitoring the fluorescence of the active site can directly probe the catalysis. The classic example of this

approach is the study of cholesterol oxidase (COx) by Xie and coworkers.²⁰ Gafni, Palfey, Steel, and coworkers further applied this approach to study dihydroorotate dehydrogenase^{63,64} and *p*-hydroxybenzoate hydroxylase.²⁴ Here, we will use the COx study to exemplify the approach.

9.21.2.2 Example: Catalytic Dynamics of Cholesterol Oxidase

COx catalyzes the oxidation of cholesterol by oxygen. The active site of the enzyme contains a flavin adenine dinucleotide (FAD), which is naturally fluorescent in its oxidized form (FAD) but not in its reduced form (FADH₂). During the catalytic cycle, the FAD at the active site is reduced to FADH₂ by the substrate cholesterol, which is then oxidized back to FAD by O₂ (**Figure 1(a)**). Therefore, each catalytic turnover of a COx is accompanied by a cycle of the active site between the fluorescent oxidized FAD form and the nonfluorescent reduced FADH₂ form. Monitoring the fluorescence of the FAD can thus directly probe the catalysis of a single COx molecule in real time.

Xie and coworkers utilized the intrinsic fluorescence properties of the FAD active site of COx to study its catalytic dynamics.²⁰ Using confocal fluorescence microscopy, they recorded real-time fluorescence intensity trajectories of single COx molecules trapped in agarose gels that also contain the substrate cholesterol and oxygen. The fluorescence trajectory of a single COx molecule shows digital on–off events where each on–off event represents a single catalytic turnover between the FAD and FADH₂ forms of the enzyme (**Figure 1(b)**). The fluorescence on-times in the trajectory are the stochastic waiting times for the reduction reaction of Enzyme–flavin adenine dinucleotide (E–FAD) and the off-times are those for the oxidation reaction of E–FADH₂. Both waiting times can be statistically analyzed to extract out the kinetics of the associated reactions. The distribution of on-times in **Figure 1(c)** exemplifies the kinetic information contained in the single-turnover waiting times: the delayed maximum of the on-time distribution reflects the presence of a kinetic intermediate during the reduction of FAD by cholesterol, which is an enzyme–substrate complex as in the classic Michaelis–Menten mechanism.

The real-time single-turnover trajectories also enabled Xie and coworkers to analyze the time-dependent activity of each enzyme molecule. They found that individual COx molecules show temporal activity fluctuations (i.e., dynamic disorder in activity), attributable to the slow conformational dynamics of the enzyme. The timescale of the activity fluctuation is the timescale of the conformational dynamics that are longer than the catalytic turnovers and can be obtained from the autocorrelation function of the waiting times (**Figure 1(d)**), which shows an exponential decay behavior versus the index of turnovers (*m*) and whose decay constant is the fluctuation timescale. This conformational dynamics–coupled enzyme catalysis is fundamental to enzyme catalysis and extremely challenging to study with traditional methods measuring the average behaviors of a population of molecules.

9.21.2.3 Features and Generality

Many enzymes use the flavin cofactor at the active site; the fluorescent active site approach can be applied to study these enzymes at the single-molecule level. Other naturally fluorescent enzymes, like those that contain NAD cofactors, can in principle be studied, although the bluer fluorescence of NAD poses a technical challenge for single-molecule fluorescence detection. As the approach uses the natural fluorescence of the enzyme, no labeling with fluorescent probes is needed, offering no or minimum perturbation on the enzyme structure and function.

9.21.2.4 Challenges

Common to most fluorescence-based single-molecule methods, photobleaching limits the observation time window using the fluorescent active site approach. For COx, its FAD cofactor showed a significantly better stability than common dye molecules, possibly due to the protection by the protein.²⁰ As this approach relies on the natural fluorescence of the enzyme, the application is largely limited to flavin enzymes. And, more often than not, the natural fluorescence of the FAD cofactor inside a protein is intrinsically quenched by nearby redox-active residues (e.g., tyrosine, tryptophan) through photo-induced electron transfer (see Section 9.21.7). This natural fluorescence quenching can sometimes be circumvented by mutating the residues that cause quenching, although caution needs to be exercised that the mutation will not perturb the enzyme function significantly.

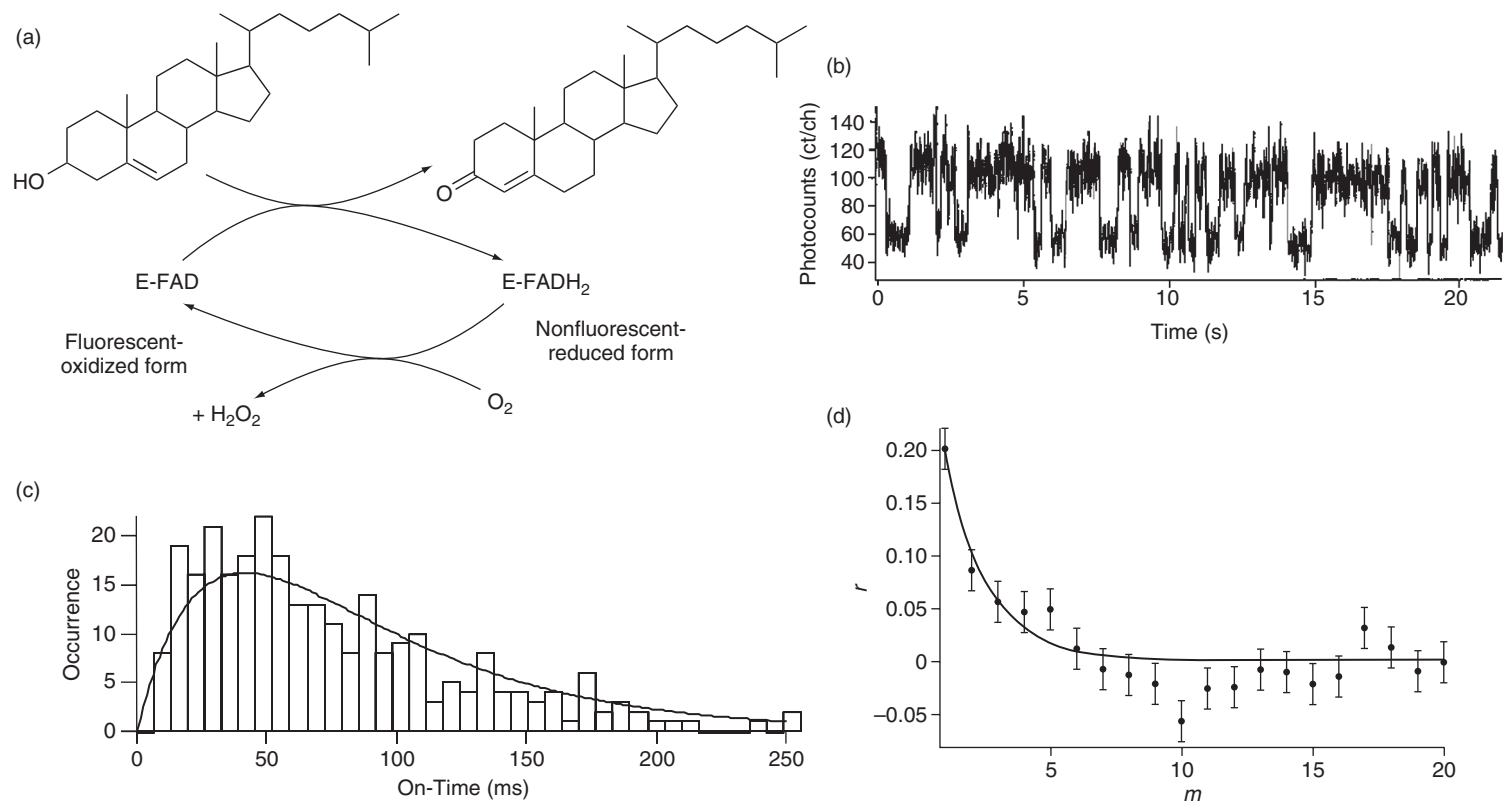


Figure 1 (a) Catalytic cycle of COx. E: enzyme. (b) Fluorescence intensity trajectory of a single COx molecule during catalysis. (c) Distribution of the on-times (bars) derived from the fluorescence intensity trajectory of a single COx molecule at 2 mmol l⁻¹ cholesterol. (d) The autocorrelation function of on-times $r(m) = \langle \Delta t(0)\Delta t(m) \rangle / \langle \Delta t^2 \rangle$; m is the index of turnovers. Reproduced from H. P. Lu; L. Y. Xun; X. S. Xie, *Science* **1998**, 282, 1877–1882. Reprinted with permission from AAAS.

9.21.3 Fluorogenic Reaction

9.21.3.1 Principle

The chemical transformation catalyzed by an enzyme also provides an opportunity to study catalysis at the single-molecule level. If this chemical transformation generates a fluorescent product (i.e., a fluorogenic reaction), monitoring the fluorescence of the product can directly probe the catalysis. This fluorogenic reaction approach is arguably the most popular in studying enzymes at the single-molecule level. Two experimental designs have been reported in applying this approach to assay single enzyme activity: one to detect the generation of every product molecule in real time by a single enzyme at single-turnover resolution,^{21–23,54–56,65–67} and the other to monitor the accumulation of all the product molecules over time produced by a single enzyme encapsulated in a confined volume.^{68–75}

Using the real-time single-turnover detection design, Rigler and coworkers first examined the activity of horseradish peroxidase at the single-molecule level,^{22,54} which was further studied by Engelkamp and coworkers.⁶⁶ Velonia *et al.*,²³ Flomenbom *et al.*,⁵⁵ and Carette *et al.*⁶⁷ used this approach to study lipase catalysis. Xie *et al.*²¹ and Moerner *et al.*⁵⁶ studied β -galactosidase, a favorite system in single-molecule enzymology studies. Hofkens and coworkers also used this to study chymotrypsin.⁶⁵ On the contrary, using encapsulation in confined volume, Yeung *et al.*⁶⁸ studied lactate dehydrogenase and Dovichi *et al.*⁶⁹ studied alkaline phosphatase by trapping individual enzymes in capillary tubes. Noji and coworkers⁷⁰ and Collier and coworkers⁷⁵ used microchambers formed in polydimethylsiloxane (PDMS) stamps, and Walt and coworkers^{71,72} used microchambers formed at the tips of optical fibers to trap individual β -galactosidase molecules for activity assays. Liposomes⁷⁴ and water-in-oil emulsions⁷³ were also used to encapsulate individual alkaline phosphatase⁷⁴ and chymotrypsin⁷³ enzymes for activity assays with fluorogenic reactions.

Here, the studies by Xie and coworkers²¹ and Noji and coworkers⁷⁰ using the fluorogenic reaction approach are used to illustrate these two experimental designs, both of which studied β -galactosidase as a model enzyme.

9.21.3.2 Example 1: β -Galactosidase with Single-Turnover Detection

β -Galactosidase (β -gal) catalyzes the hydrolysis of lactose. A nonfluorescent substrate resorufin- β -D-galactopyranoside (RGP) can be hydrolyzed by β -gal to generate the fluorescent resorufin (R) as one of the reaction products (Figure 2(a)). Using this fluorogenic reaction, Xie and coworkers studied the enzyme kinetics of individual β -gal molecules in real time at single-turnover resolution.²¹ To follow the catalysis of a single β -gal molecule, they immobilized the enzyme onto polystyrene beads, which are in turn immobilized on a glass surface, and monitored the fluorescence signal from a single β -gal molecule in real time using confocal fluorescence microscopy (Figure 2(a)). The micron-sized beads are visually identifiable under an optical microscope, helping to locate individual β -gal molecules. The fluorescence intensity trajectory from a single β -gal molecule shows stochastic fluorescence bursts in the presence of the substrate RGP; each burst represents a single turnover of catalytic product formation (Figure 2(b)). The intervals between any two neighboring fluorescence bursts are the microscopic waiting times (τ) for individual product formation events, and these waiting times are the most important observables in the trajectory and contain most information about the catalytic dynamics.

Since each catalytic reaction generates a new product molecule, the fluorogenic reaction approach is not limited by photobleaching and long turnover trajectories can be obtained. Counting the burst frequency in sequential time segments of a single trajectory directly determines the time evolution of the activity of a single β -gal molecule (Figure 2(c)). The activity of a single β -gal molecule shows strikingly temporal fluctuations that occur over a wide range of timescales. This temporal activity fluctuation is especially significant at high substrate concentrations where the catalytic conversion reaction is rate-limiting in the overall turnover cycle (Figure 2(c), blue trajectory), indicating the large fluctuation of the catalytic rate constant of the enzyme. This dynamic fluctuation of enzyme activity, that is, dynamic disorder, is attributable to the interconversion dynamics of different enzyme conformers that have different activities. Xie and coworkers further showed that the classic Michaelis–Menten still holds for fluctuating single enzymes, as shown by the Lineweaver–Burke plot of $\langle\tau\rangle$ versus $1/[S]$, where $\langle\tau\rangle$ is the time average of single-turnover waiting times (Figure 2(d)).

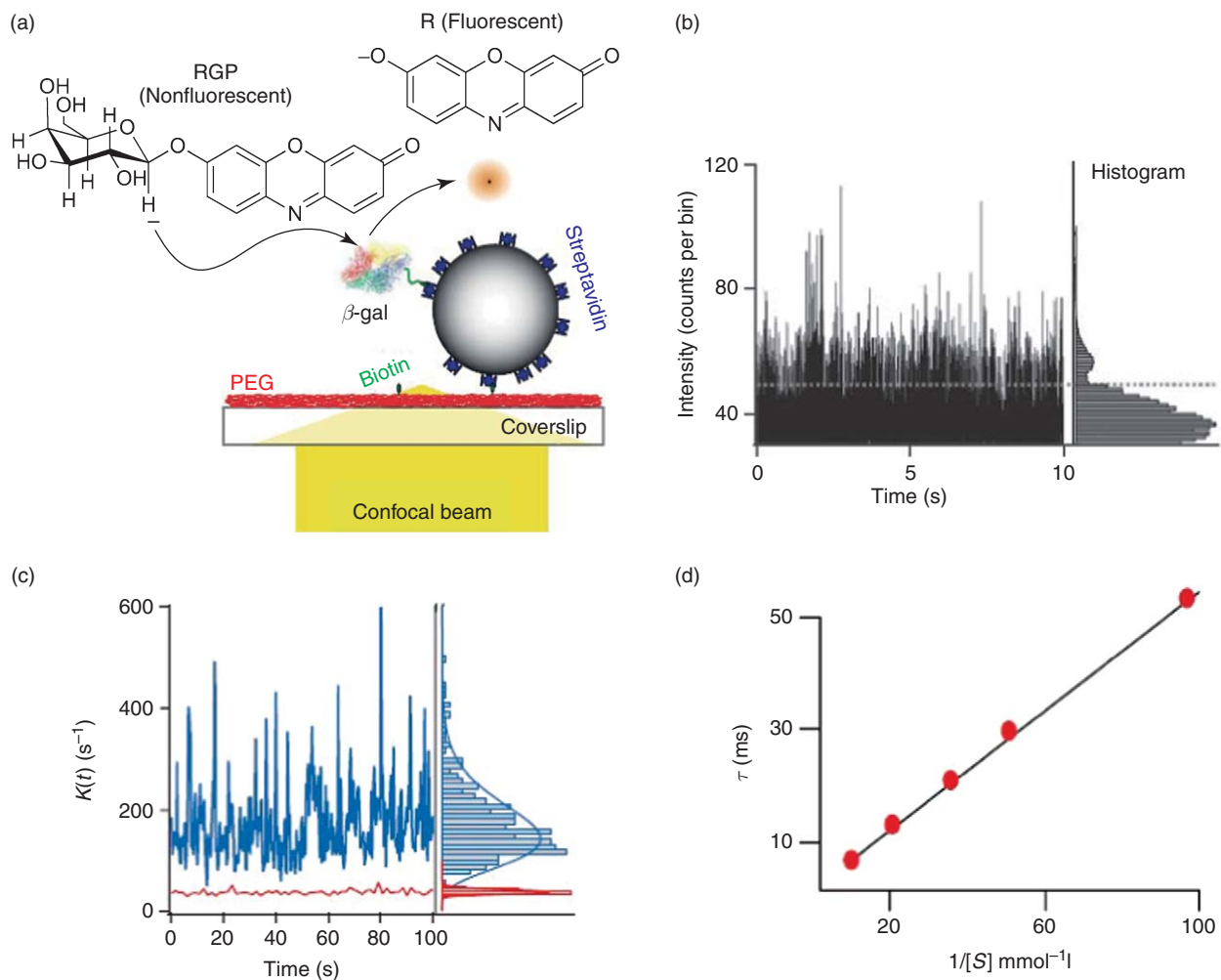


Figure 2 (a) Schematic of enzyme immobilization and fluorescence detection. A single β -gal molecule is linked to a streptavidin-coated polystyrene bead, which is immobilized on a biotin-coated glass surface. RGP: resorfin- β -D-galactopyranoside; R: resorfin. (b) Fluorescence intensity trajectory of a single β -gal molecule at $100 \mu\text{mol l}^{-1}$ RGP. Dashed line is the threshold separating the signal from the background noise. On the right is the fluorescence intensity histogram. (c) Two trajectories of turnover rates $k(t)$ of two β -gal enzymes at $20 \mu\text{mol l}^{-1}$ (red) and $100 \mu\text{mol l}^{-1}$ (blue) RGP concentration. On the right are the corresponding histograms of $k(t)$. (d) Single-molecule Lineweaver-Burke plot, $\langle \tau \rangle$ versus $1/[S]$. The line is a fit with the classic Michaelis-Menten equation. Reprinted by permission from Macmillan Publishers Ltd: B. P. English; W. Min; A. M. van Oijen; K. T. Lee; G. Luo; Y. Sun; B. J. Cherayil; S. C. Kou; X. S. Xie, *Nat. Chem. Biol.* **2006**, 2, 87-94, copyright (2006).

9.21.3.3 Example 2: β -Galactosidase with Microchamber Encapsulation

Although the real-time single-turnover detection is powerful with fluorogenic reactions, a few challenges still exist under certain circumstances. First, for enzymes having slow overall turnover rates but fast product dissociation, one needs to maintain a 'short' time resolution in fluorescence detection to catch every product molecule before it dissociates from the enzyme and at the same time needs to monitor the same enzyme for a 'long' time to observe statistically significant number of turnover events. This broad time range poses a technical challenge in practice, because maintaining high time resolution for a long period will generate trajectories with a huge number of data points that often push the capacity of computers. Second, surface immobilization sometimes affects the enzyme activity significantly. Third, the nonfluorescent substrates for fluorogenic reactions still have some fluorescence (although weak), and the experiments are often limited to the relatively low concentration range of substrates to achieve single-molecule sensitivity of the product molecule.

Encapsulation of single enzyme molecule in confined volumes offers a way to overcome these challenges. By trapping a single enzyme molecule in a confined volume with substrates inside, the product will be confined in the same volume and its accumulation over time can be detected without maintaining a high time resolution to catch the product. Immobilization is also unnecessary due to confinement. Moreover, as one can monitor the accumulation of many product molecules produced by a single enzyme in the same confined volume, high substrate concentration conditions can also be studied without worrying about suppressing background for single-molecule detection.

This confined volume strategy is well demonstrated by the microchamber encapsulation work by Noji and coworkers.⁷⁰ Using soft-lithography, they fabricated arrays of femtoliter microchambers on a PDMS stamp (Figure 3(a)). They then encapsulated enzyme–substrate solutions in these microchambers, and kept the enzyme concentration low (picomolar–nanomolar) to ensure statistically there would be one or two enzyme molecules in each microchamber. They studied β -gal as a model system and used fluorescein-di- β -galactopyranoside as the fluorogenic substrate that will generate fluorescein as a product. Imaged by a wide-field fluorescence microscope that can observe many microchambers simultaneously, the enzyme activity is manifested by the steady increase of fluorescence intensity inside individual microchambers, reporting the product accumulation because of enzyme catalysis (Figure 3(b)). The characteristic of single-enzyme catalysis is the discrete sloping of the fluorescence intensity versus time trajectories; the discrete sloping here results from the discrete number of enzyme molecules in each microchamber (i.e., zero, one, or two enzymes) (Figure 3(b)). From these slopes, the rate of product accumulation can be derived for the catalysis in each microchamber. The histogram of the rates from many microchambers shows multiple peaks, corresponding to microchambers that contain zero, one, two, and three enzyme molecules (the distribution here follows the Poisson distribution).

9.21.3.4 Features and Generality

As the fluorescent product is continuously generated during catalysis, the biggest advantage of the fluorogenic reaction approach is that there is no photobleaching limit, which is common to many other fluorescence-based single-molecule techniques. The nonfluorescent (or weakly fluorescent) nature of the substrate also enables study over a wide range of substrate concentrations; even for high substrate concentrations where the increased background prevents single-molecule product detection, the confined-volume strategy still allows study of single enzyme catalysis. As no fluorescent labeling of the enzyme is involved, there is no perturbation on the enzyme function.

The fluorogenic reaction approach is also widely applicable so long as suitable fluorogenic reactions are available. With modern synthetic methods, suitable fluorogenic substrates can probably always be designed and synthesized for a particular enzymatic reaction; examples are already available in the literature.^{76–80}

9.21.3.5 Challenges

To study a particular enzyme using the fluorogenic reaction approach, the first challenge is to find a fluorogenic substrate. As discussed above, with modern synthetic chemistry, the availability of suitable substrates is only limited by researchers' creativity in designing molecules.

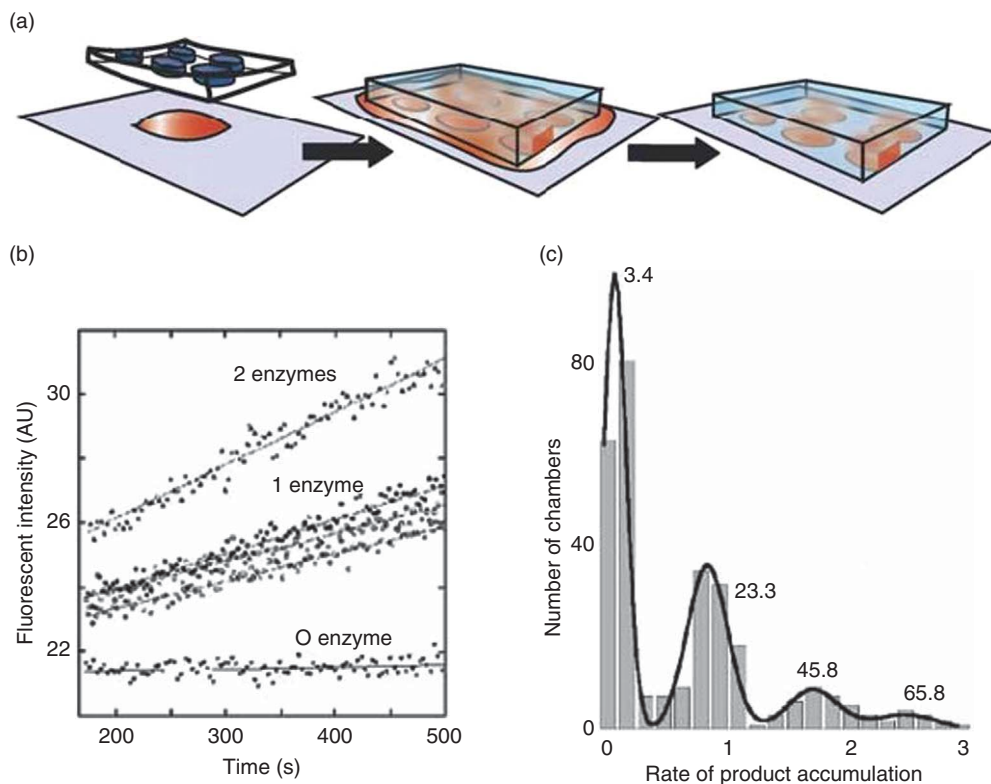


Figure 3 (a) Schematic of solution encapsulation by PDMS stamps with embedded femtoliter microchambers. (b) Exemplary fluorescence intensity versus time trajectories from individual microchambers. The time resolution here is much longer than the turnover time. The different slopes reflect the different number of enzyme molecules in each microchamber. (c) Histogram of product accumulation rates from many microchambers. From low to high values, the multiple peaks correspond to microchambers containing zero, one, two, and three enzyme molecules, respectively. Reprinted by permission from Macmillan Publishers Ltd: Y. Rondelez; G. Tresset; K. V. Tabata; H. Arata; H. Fujita; S. Takeuchi; H. Noji, *Nat. Biotechnol.* **2005**, *23*, 361–365, copyright (2005).

For the real-time single-turnover detection of fluorogenic reactions, catalytic reactions with fast turnover rates (or fast product dissociation) pose a time resolution challenge, as single-molecule fluorescence detection often requires detection of hundreds of photons to obtain statistically significant information. For these fast enzymes, one can vary the substrates, use enzyme variants from different organisms, or use mutants to slow the catalysis down.

For the encapsulation in confined volume strategy, the observation time is limited by the total amount of substrate molecules available in the enclosed chambers, and the catalysis ends when all substrate molecules are consumed. Therefore, it is desirable to have free exchange of reaction solutions. For the PDMS-based microchambers, one way is to couple the microchambers to microfluidic channels, which allow solution exchange and are controllable through pressure valves, as demonstrated by Collier and coworkers.⁷⁵

9.21.4 Fluorescent Substrate

9.21.4.1 Principle

Besides detecting the fluorescence of the catalytic product, another approach to study enzymes at the single-molecule level is to detect the fluorescence of the substrate. Here, the substrate, either naturally fluorescent or fluorescently labeled, is monitored at the single-molecule level to directly follow its association with the

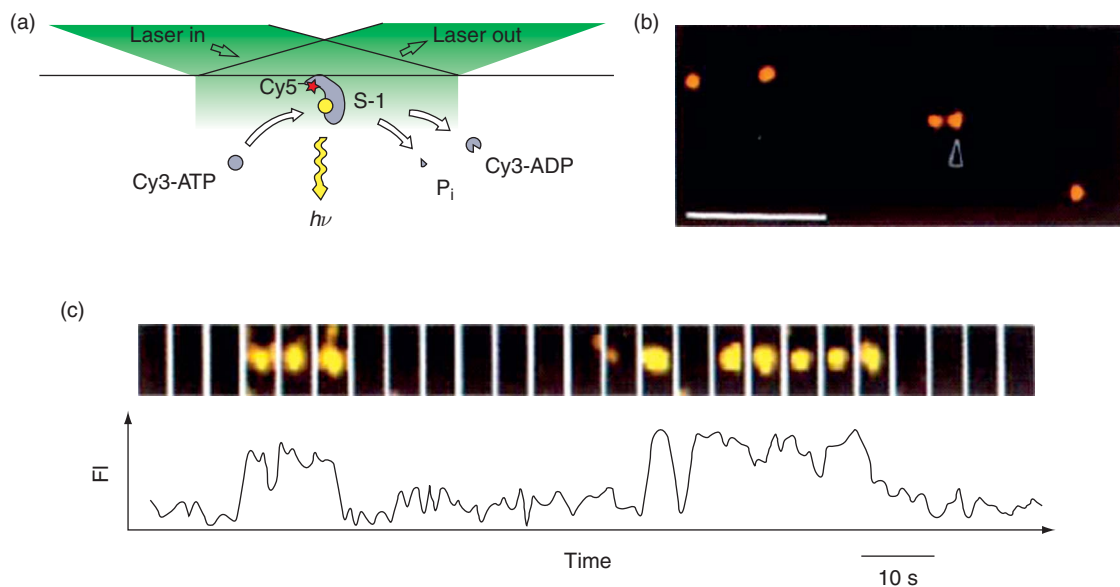


Figure 4 (a) Schematic of experimental design of detecting single-head myosin catalysis using a fluorescent substrate. The laser excitation is in TIR geometry. The Cy5-label on the enzyme helps to identify the location of individual enzymes. (b) Fluorescence image of Cy5-labeled myosin immobilized on the surface under solution. Cy5 is excited at 632 nm. The image is artificially colored red. (c) ATP turnovers by a single myosin molecule. The upper panel shows typical fluorescence images of Cy3-nucleotide (ATP or ADP) coming in and out of focus by associating and dissociating with a myosin molecule marked by an arrowhead in (b). Cy3-fluorescence is excited at 532 nm. The image is artificially colored yellow. The lower panel shows the time trajectory of the corresponding fluorescence intensity. Figure (a) reprinted with permission from Macmillan Publishers Ltd: T. Funatsu; Y. Harada; M. Tokunaga; K. Saito; T. Yanagida, *Nature* **1995**, 374, 555–559, copyright (1995).

enzyme and the subsequent dissociation. Yanagida and coworkers used this approach to detect the ATP hydrolysis activity of single myosin molecules,^{61,81} which is described below.

Myosin is a motor protein and hydrolyzes ATP to power its mechanical movement along actin filaments. The ATP hydrolysis comes from the ATPase activity of the myosin molecule. Yanagida and coworkers used the fluorescent substrate approach to visualize its ATPase activity at the single-molecule level.^{61,81} They synthesized a Cy3-dye-labeled ATP derivative, Cy3-ATP, as a fluorescent substrate for myosin. To monitor the ATP hydrolysis turnovers by single myosin molecules, they immobilized myosin molecules on a glass surface (**Figure 4(a)**). The myosin was labeled with a Cy5-dye to facilitate its identification. They first obtained the Cy5-fluorescence image to locate individual myosin molecules immobilized on the glass surface using TIR fluorescence microscopy and 632-nm excitation (**Figure 4(a,b)**). The Cy3-ATP substrate was supplied in the solution. They then switched to a 532-nm laser to directly excite the Cy3-fluorescence to probe the ATP hydrolysis by single myosin molecules. Each association event of a Cy3-ATP molecule to the enzyme is reported by a sudden appearance of the Cy3-fluorescence signal at the position of a myosin molecule; the subsequent dissociation of the hydrolyzed product Cy3-ADP or unhydrolyzed substrate is reported by the sudden disappearance of the Cy3-fluorescence (**Figure 4(c)**). By analyzing the distribution of the fluorescence residence times, that is, the on-times in the Cy3-fluorescence intensity trajectories (**Figure 4(c)**), they were able to determine the dissociation rate that agrees with the ATP turnover rate of Cy3-ATP by myosin.

9.21.4.2 Features and Generality

The fluorescent substrate approach is in principle generalizable, if suitable fluorescent substrates are available. As the fluorescence signal is associated with the substrate, substrate binding to the enzyme is directly observable, and so is the lifetime of enzyme–substrate complex (possibly including the lifetime of the

enzyme–product complex if the product also carries the same fluorescence). The direct observation of substrate actions is advantageous compared to the fluorogenic reaction approach, which cannot observe substrate binding to the enzyme. This approach is also not limited by photobleaching, because the fluorescent substrate can be supplied continuously with solution flow and typical photobleaching lifetimes of fluorescent probes are longer than the substrate residence time on the enzyme.

9.21.4.3 Challenges

A big limitation of the fluorescent substrate approach is the concentration limit – because the substrate is fluorescent, the experiments have to be done at low substrate concentrations (10^{-12} – 10^{-9} mol l⁻¹) to suppress the fluorescence background for single-molecule detection. (The TIR scheme in Yanagida and coworker's study^{61,81} helps suppress the background owing to the small excitation volume.) At these low concentrations, enzyme turnover rate is often diffusion limited. Moreover, because the fluorescence signal is associated with the substrate, whether the chemical transformation of catalysis has indeed happened is unclear, and the disappearance of the signal could simply result from substrate dissociation, not dissociation of the catalytic product. Supplementary experiments are needed here to confirm that catalysis does happen at the single-molecule imaging conditions.

9.21.5 Fluorescence Resonance Energy Transfer (FRET)

9.21.5.1 Principle

FRET is widely applied in single-molecule fluorescence studies of biomolecules.^{31,32,82} Governed by the Förster mechanism,⁸³ the spectral overlap between the fluorescence spectrum of a donor molecule and the absorption spectrum of an acceptor can result in efficient energy transfer from the donor to the acceptor. The energy transfer efficiency is dependent on the donor to acceptor distance, r , within the nanometer range (energy transfer efficiency = $1/[1+(r/r_0)^6]$, where r_0 is the Förster radius of the donor–acceptor pair, a constant typically of a few nanometers^{83,84}). The most general experimental design of applying FRET is to label biomolecules with a fluorescent donor–acceptor pair and then monitor the fluorescence intensities of both the donor and the acceptor at the single-molecule level. For studying enzymes, if an enzyme reaction involves nanometer-scale distance changes between any parts of the enzyme complex, the enzyme reaction can be studied by the single-molecule FRET method by labeling the enzyme (or the enzyme complex) with a pair of FRET probes at appropriate locations.

Weiss and coworkers pioneered in using single-molecule FRET to study the conformational dynamics and reaction mechanism of staphylococcal nuclease.⁸⁵ Lu and coworkers used it to study the conformational dynamics of T4 lysozyme during catalysis.⁵⁸ Hammes, Benkovic, and coworkers studied dihydrofolate reductase,²⁵ the enzymes involved in T4 primosome⁸⁶ and replisome.^{87,88} Yang and coworkers studied adenylate kinase.⁸⁹ Here, we use the T4 lysozyme study to illustrate the approach.⁵⁸

9.21.5.2 Example: Conformational Dynamics-Coupled Catalysis of T4 Lysozyme

T4 lysozyme catalyzes the hydrolysis of polysaccharide chains of *E. coli* cell wall matrices. This enzyme has two domains connected by an α -helix (Figure 5(a)), and the active site sits between the two domains. During catalysis, the two domains undergo hinge-bending motions that are coupled with substrate binding. Lu and coworkers used single-molecule FRET to study this conformational dynamics of T4 lysozyme under hydrolysis reactions.⁵⁸ They attached a FRET donor–acceptor pair, tetramethylrhodamine (TMR) and Texas Red, to Cys54 and Cys97 of the enzyme. By exploiting the reactivity difference of maleimide and iodoacetamide with the sterically constrained Cys54, they were able to label these two cysteines with TMR and Texas Red site specifically. At these two labeling positions, the TMR–Texas Red interdistance directly reports the hinge-bending motions of the two domains of the lysozyme. With a Förster radius of ~ 50 Å for this FRET pair and an average Cys54–Cys97 distance of ~ 36 Å, the energy transfer from TMR to Texas Red is sensitive to their interdistance changes from the enzyme conformational dynamics.

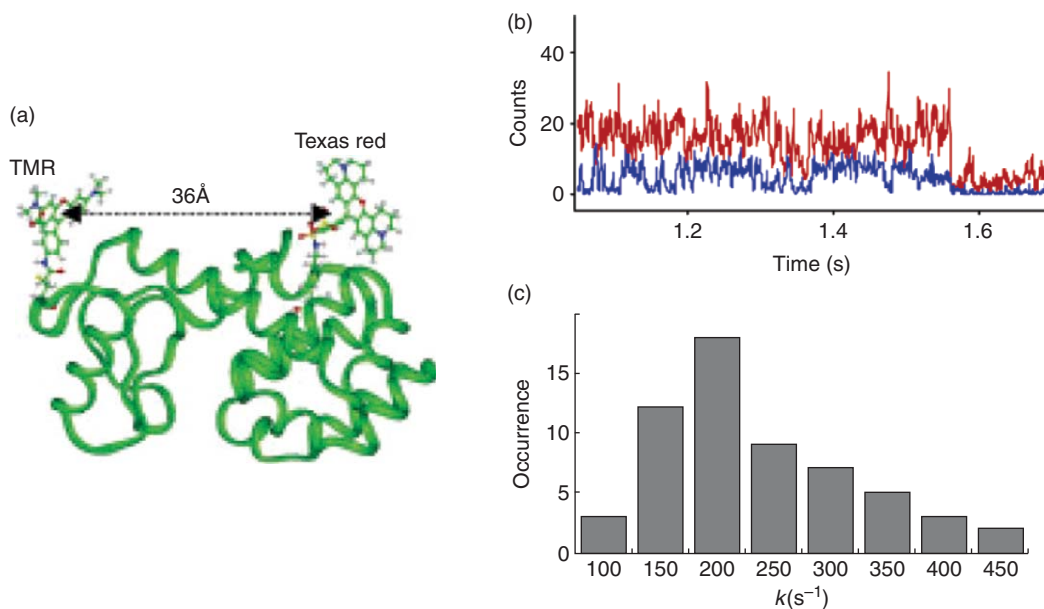


Figure 5 (a) The structure of T4 lysozyme with the two dye labels schematically shown. (b) Fluorescence intensity trajectories of the TMR donor (blue) and the Texas Red acceptor (red) of a single T4 lysozyme in the presence of *E. coli* B cell wall. (c) Distribution of the decay rate constants (k) of the donor intensity autocorrelation functions. Reproduced with permission from Y. Chen; D. Hu; E. R. Vorpagel; H. P. Lu, *J. Phys. Chem. B.* **2003**, *107*, 7947–7956. Copyright (2003) American Chemical Society.

To follow the conformational dynamics of T4 lysozyme, Lu and coworkers used confocal fluorescence microscopy to monitor the real-time energy transfer between the two probes on a single enzyme molecule by monitoring the fluorescence intensities of both probes.⁵⁸ The donor–acceptor fluorescence intensities of a single lysozyme show large anticorrelated fluctuations in the presence of the substrate (i.e., *E. coli* cell wall), directly reporting the enzyme conformational dynamics (Figure 5(b)). By analyzing the autocorrelations of the fluorescence intensity trajectories, they determined the rate constant of the conformational dynamics for individual enzymes. They observed large static heterogeneity in the distribution of the rate constant (Figure 5(c)), indicating the widely varying dynamic properties of individual enzyme molecules. The large static heterogeneity was attributed to enzyme searching for reactive sites on the substrate.

9.21.5.3 Features and Generality

FRET is a general approach for studying enzymes. So long as there are structural changes within the enzyme or the enzyme complex during catalysis, FRET can be used to monitor the conformational dynamics and thus the enzyme reaction. A wide variety of fluorescent probes are available.⁸⁴ With different combinations of these probes, FRET pairs of different Förster radii can be designed to cover a large range of distances.

9.21.5.4 Challenges

As FRET methods require a pair of fluorescent probes, to label a protein with two probes site-specifically is a general challenge. Orthogonal labeling chemistry is needed to place the donor and the acceptor at the specific locations. Luckily, for many occasions, one merely needs to label the enzymes with two labels at two locations, obtaining a mixture of donor–donor-, acceptor–acceptor-, donor–acceptor-, and acceptor–donor-labeled molecules. Under single-molecule imaging conditions, the donor–donor- and acceptor–acceptor-labeled molecules are easily distinguishable and discarded; and the donor–acceptor and acceptor–donor-labeled ones are often effectively the same for FRET measurements.

Based on the Förster mechanism and the available probes suitable for simultaneous single-molecule two-color detection, the sensitivity of FRET is limited to nanometer-scale conformational changes. Angstrom-scale conformational changes, which are also common for biomacromolecules, are beyond the sensitivity of FRET. For detecting angstrom-scale dynamics, the fluorescence quenching via electron transfer provides an alternative (see Section 9.21.7). Engineering biomolecules to amplify small-scale structural changes is a viable strategy to enable single-molecule FRET measurements, such as our work of using engineered DNA Holliday junctions to study protein–DNA interactions that involve merely small structural changes. Photobleaching also limits the observation time of FRET measurements. Nonetheless, with a good oxygen scavenging system, a single fluorescent probe molecule can last for up to a few minutes before being photobleached;⁹⁰ complication here is that the O₂ scavenging system must not interfere with the enzyme reaction.

9.21.6 Fluorescence Quenching via Energy Transfer

9.21.6.1 Principle

Instead of using a pair of donor–acceptor fluorescent probes, a variant of FRET, fluorescence quenching via energy transfer, uses only one fluorescent probe as a donor. The acceptor is nonfluorescent and acts as a quencher – it has strong absorption bands that overlap spectrally with the fluorescence of the donor. This energy-transfer-caused quenching changes the donor fluorescence, from which the chemical state of the acceptor (i.e., quencher) or the distance between the donor and the quencher can be deduced. Hammes and coworkers used this fluorescence quenching approach to examine the substrate binding and catalysis of dihydrofolate reductase.^{59,60} Visser and coworkers used this approach to probe the catalysis of *p*-hydroxybenzoate hydroxylase.⁹¹ Also, Canters and coworkers used this to follow the reaction of nitrite reductase (NiR).⁹² Here, we use the NiR study to exemplify the approach.

9.21.6.2 Example: Catalysis of Nitrite Reductase

NiR catalyzes the reduction of nitrite (NO₂[−]) to nitric oxide (NO). The enzyme is a homotrimer (**Figure 6(a)**); each monomer contains two mononuclear copper sites: one so-called type-1 copper site that acts as an electron transfer center and the other so-called type-2 copper site where the catalysis occurs. These two copper sites have distinct absorption properties. The type-1 site belongs to the large family of blue copper sites in biology and has a cysteine ligand. At the oxidized form (Cu²⁺), this cysteine ligand gives rise to an intense sulfur-to-Cu²⁺ charge transfer absorption near 600 nm ($\epsilon > 4000 \text{ mol}^{-1} \text{ l cm}^{-1}$); at the reduced form (Cu¹⁺), this site has no absorption in the visible region because of the d¹⁰ electron configuration of Cu¹⁺ ions. On the contrary, the type-2 copper site has histidine and water-based ligands and shows little or no absorption in the visible region regardless of its oxidation state.

Canters and coworkers utilized the different spectral features between the oxidized and reduced forms of the type-1 copper site to follow NiR catalysis at the single-molecule level.⁹² They labeled one monomer of NiR at the N-terminus with the fluorescent probe ATTO-655, whose fluorescent spectrum overlaps with the absorption band of the oxidized type-1 copper site. Because of this spectral overlap, the fluorescence intensity of ATTO-655 is quenched by energy transfer to the type-1 copper site when this copper site is at the oxidized form. If the type-1 copper site is at the reduced form, no quenching via energy transfer occurs and the fluorescence intensity of ATTO-655 is high. During the catalysis of NiR, its type-1 copper site cycles through oxidized and reduced forms repetitively, and the ATTO-655 consequently undergoes quenching and no-quenching, resulting in its temporal fluorescence intensity fluctuations that are coupled with the catalysis (**Figure 6(a)**). Based on this scheme, Canters and coworkers used confocal fluorescence microscopy to monitor the real-time catalysis of surface-immobilized NiR molecules at the single-molecule level. They observed large fluorescence intensity fluctuations that report the turnover dynamics of individual NiR molecules (**Figure 6(b)**). By analyzing the fluctuation behaviors of individual trajectories, they revealed a distribution of electron transfer rates between the type-1 and type-2 copper centers during the catalytic cycle, which is related to the disorder of the catalytic site of the enzyme.

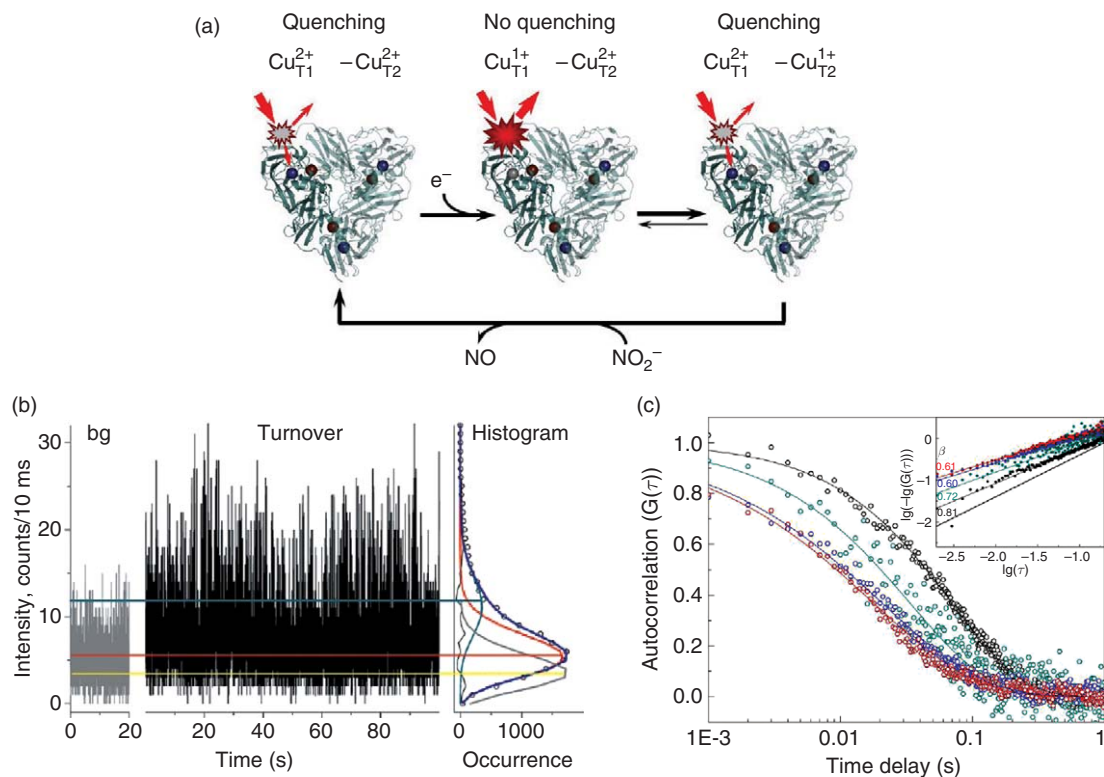


Figure 6 (a) Schematic of sequence of events during turnover of a labeled NiR, showing the fluorescence quenching via energy transfer that reports the turnover. Left: the resting enzyme, both type-1 Cu (Cu_{T1}, blue) and type-2 Cu (Cu_{T2}, red) are at the 2+ oxidized state Cu_{T1}²⁺–Cu_{T2}²⁺, and fluorescence of the label is low due to fluorescence quenching via energy transfer to the oxidized Cu_{T1}²⁺. Center: upon reduction of Cu_{T1} by an external reductant, the label fluorescence increases, due to the disappearance of energy transfer from the label to the reduced Cu_{T1}¹⁺ (gray). Right: An electron is transferred to from Cu_{T1} to Cu_{T2}, which becomes reduced (gray); the label fluorescence is again quenched by the oxidized Cu_{T1}²⁺. (b) Fluorescence intensity trajectory of a single labeled NiR enzyme undergoing catalysis ('turnover'), in comparison with that in the absence of catalysis ('bg'). The corresponding fluorescence intensity histogram is shown on the right. (c) Fluorescence intensity autocorrelation functions of individual NiR enzymes at 5 μmol l⁻¹ (black), 50 μmol l⁻¹ (green), 500 μmol l⁻¹ (blue), and 5 mmol l⁻¹ (red) NaNO₂. Normalized data (circles) were fitted with stretched exponential functions (lines), $G(t) = \exp(-(t/\tau_0)^\beta)$. Inset: same curves plotted as $\log(-\log(G(t)))$ versus $\log(t)$. Reproduced with permission from S. Kuznetsova; G. Zauner; T. Aartsma; H. Engelkamp; N. Hatzakis; A. E. Rowan; R. J. M. Nolte; P. C. M. Christianen; G. W. Canters, *Proc. Natl. Acad. Sci. U.S.A.* **2008**, *105*, 3250–3255; Copyright (2008) National Academy of Sciences, U.S.A.

9.21.6.3 Features and Generality

The fluorescence quenching via energy transfer approach could be widely applicable for studying many other enzymes. In principle, any enzyme that has active sites with intense absorption properties can be targeted using this approach. In particular, for metalloenzymes, which use transition metals at the active site (e.g., NiR), the metal-based catalysis often involves species that have intense ligand-to-metal charge transfer absorptions.⁹³ These strong chromophoric species can be exploited as quenching centers for single-molecule fluorescence detection.

The use of external fluorescent probes is also general. Site-specific labeling of proteins is readily achievable with many accessible labeling schemes including site-directed mutagenesis, green fluorescent protein (GFP) fusion, and unnatural amino acids.^{84,94} Many fluorescent probes suitable for single-molecule detections are also available covering a wide spectral range.⁸⁴ Besides targeting the enzyme active site as a quencher, such as in the study of NiR⁹² and *p*-hydroxybenzoate hydroxylase,⁹¹ chromophoric substrates can also act as a quencher for this scheme, as demonstrated in the study of dihydrofolate reductase.^{59,60}

9.21.6.4 Challenges

Common to most fluorescence-based single-molecule methods, photobleaching limits the observation time window using the fluorescence quenching via energy transfer approach. In addition, this approach only obtains the fluorescence intensity from one probe; thus, fluorescence intensity fluctuations due to probe photophysics, such as fluorescence blinking, can complicate the results and data analyses. Triplet quenchers such as Trolox^{®95} can reduce fluorescence blinking. Careful control experiments are in any case necessary.

9.21.7 Fluorescence Quenching via Electron Transfer

9.21.7.1 Principle

A molecule at excited states often has different redox potentials from that at its ground state, and photo-induced reduction (or oxidation) of a molecule via electron transfer with another reductant (or oxidant) frequently occurs. For a fluorescent molecule, photo-induced electron transfer at an excited state can significantly shorten its fluorescence lifetime and quench its fluorescence intensity. This fluorescence quenching via electron transfer can be utilized to study enzymes on a single-molecule basis. Xie and coworkers^{96,97} have used this single-molecule approach to probe the conformational dynamics of a flavin reductase (Fre),⁹⁶ as well as the conformation dynamics of an antibody–antigen complex.⁹⁷ Sauer and coworkers also have incorporated this strategy into molecular beacons to detect nucleic acids.^{98,99} Here, we use the Fre study to exemplify the approach.

9.21.7.2 Example: Conformational Dynamics of Flavin Reductase

Fre binds a naturally fluorescent FAD cofactor tightly (**Figure 7(a)**). Upon photoexcitation, the protein-bound FAD becomes reduced by a nearby tyrosine residue (Tyr35) forming a transient charge-transferred state (**Figure 7(b)**).⁹⁶ The separated charges then quickly recombine, and the Fre–FAD complex returns to the ground state. The photo-induced electron transfer from Tyr35 to FAD significantly shortens the fluorescence lifetime, γ^{-1} , of FAD ($\gamma^{-1} = 1/(k_r + k_{nr} + k_{ET}) \approx 1/k_{ET}$, when $k_{ET} \gg k_r$ and k_{nr} ; k_r , the radiative decay rate; k_{nr} , the nonradiative decay rate; k_{ET} , the electron transfer rate), which leads to quenching of the FAD fluorescence. The electron transfer rate, k_{ET} , is exponentially dependent on and thus highly sensitive to the distance, r , between the electron donor and the acceptor ($k_{ET} = k_0 \exp(-\beta r)$, k_0 is a constant, $\beta \approx 1.4 \text{ \AA}^{-1}$ for electron transfer in proteins¹⁰⁰). Fluctuations of r due to conformational dynamics of the protein will thus cause fluctuations of k_{ET} and of γ^{-1} . Consequently, monitoring the time-dependent changes of γ^{-1} of the FAD cofactor can probe the FAD–Tyr35 distance fluctuations and the conformation dynamics of Fre on a single-molecule basis.

Xie and coworkers measured the real-time fluctuations of γ^{-1} of single Fre–FAD complexes using a time-stamped photon-by-photon detection technique, which registers the arrival time of each emitted photon and the delay time between each detected fluorescence photon and the corresponding excitation laser pulse.⁹⁶ They found that γ^{-1} of FAD in a Fre–FAD complex fluctuates over time (**Figure 7(c)**). Autocorrelation analysis indicates that the fluctuation of the fluorescence lifetime of a single Fre–FAD complex occurs at a broad range of timescales, from hundreds of microseconds to tens of seconds (**Figure 7(d)**). The broad time range of fluctuation suggests the existence of multiple interconverting conformers of a Fre–FAD complex on a rugged energy landscape, and the interconversions can be described by an anomalous diffusion model (**Figure 7(d)**). The existence of these interconverting conformers also relates to the fluctuating catalytic reactivity of the flavin enzyme COx, discussed earlier in this review.²⁰

9.21.7.3 Features and Generality

Because the electron transfer rate decays rapidly over a few angstroms, the fluorescence quenching via electron transfer approach is sensitive to subtle distance changes on the angstrom scale. This distance range is complementary to that of the widely used FRET-based techniques, such as FRET and fluorescence quenching

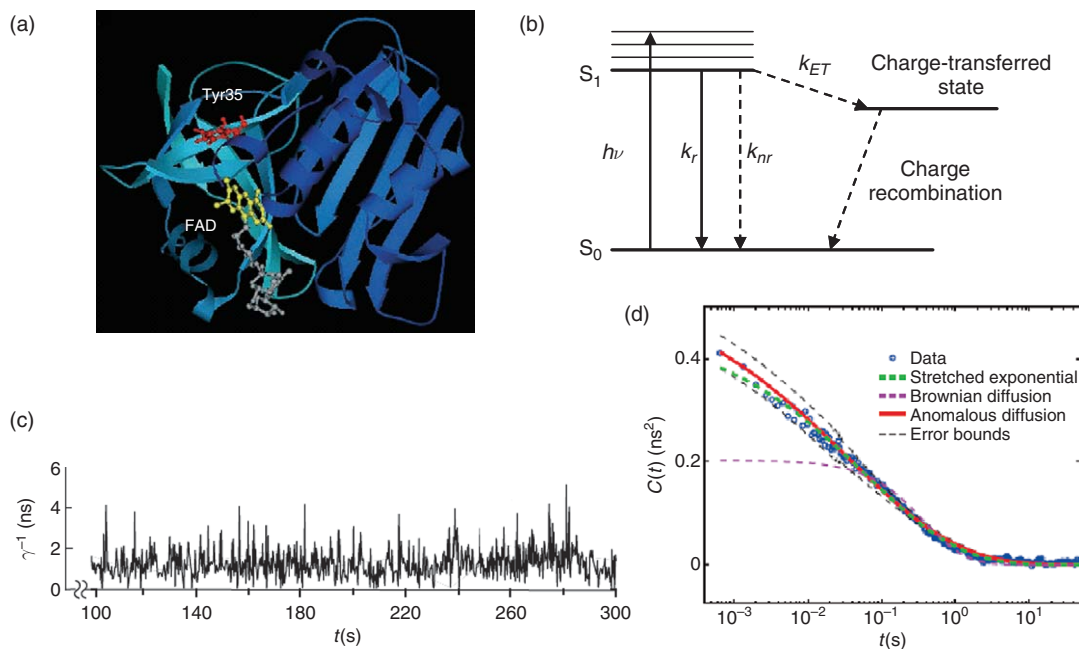


Figure 7 (a) Structure of the Fre–FAD complex. The FAD and tyrosine-35 are highlighted. (b) Energy diagram and transition schemes for the fluorescence quenching via photo-induced electron transfer process. k_r : radiative decay rate; k_{nr} , all other nonradiative decay rate; k_{ET} , electron transfer rate. (c) Trajectory of the fluorescence lifetime of a Fre–FAD complex, indicating the fluctuations of the fluorescence lifetime. (d) Autocorrelation function of the fluorescence lifetime fluctuations of a single Fre–FAD complex and fits with different models. Figures (b–d) reproduced from H. Yang; G. Luo; P. Karnchanaphanurach; T.-M. Louie; I. Rech; S. Cova; L. Xun; X. S. Xie, *Science* **2003**, 302, 262–266. Reprinted with permission from AAAS.

via energy transfer discussed in Sections 9.21.5 and 9.21.6, which are effective in studying nanometer-scale distance changes. Many structural changes in biology, for example, the geometry reorganizations of the metal active sites in redox-active enzymes, are in the angstrom range.⁹³ The fluorescence quenching via electron transfer approach offers an opportunity to study these types of structural dynamics at the single-molecule level.

The fluorescence quenching via electron transfer needs two redox-active centers: one as a quencher and the other as a probe that is also fluorescent. For the quencher, there are organic redox-active groups (e.g., tyrosine, tryptophan, and guanine) as well as metal active sites in biology that have rich redox properties and cover a broad range of redox potentials.⁹³ For the probe, in addition to the naturally fluorescent cofactors, such as FAD and flavin mononucleotide (FMN), one could label proteins externally with fluorescent probes that can undergo photo-induced electron transfer. With careful experimental design, the fluorescence quenching via electron transfer approach could have applications in many systems.

9.21.7.4 Challenges

The fluorescence quenching via electron transfer approach is also limited by photobleaching and complicated by the intrinsic photophysics of the fluorescent probe, as mentioned previously. Competition with fluorescence quenching via energy transfer can also be a problem. For example, the oxidized form of flavin, the oxidized blue copper centers, and cytochromes, all have strong absorption features and can act as a quencher via energy transfer. Selecting fluorescent probes that have fluorescence emission well separated spectrally from the absorption spectra of the quencher can circumvent this problem. Because the photo-induced electron transfer quenches the probe's fluorescence, the low detectable photon number and the shortened fluorescence lifetime of the probe are also challenges. High quantum yield (>30%) and fast response (<100 ps) detectors are needed to detect the weak fluorescence and resolve the short photon delay time in the photon-by-photon approach.⁹⁶ To use an externally introduced fluorescent probe to measure angstrom-scale distance changes, the attachment

of the probe is critical. The probe needs to be anchored to the protein rigidly so its conformational flexibility around the attachment point will not overwhelm the measurements of the angstrom-scale protein conformational dynamics. Although there are many challenges in using the fluorescence quenching via electron transfer approach, we think that the rich redox properties in redox-active enzymes make it attractive to explore this approach for more applications and discoveries.

9.21.8 Summary

With the continuing development and application of single-molecule methods, more single-molecule enzyme studies are to follow. Here, we have reviewed single-molecule fluorescence methods in studying enzymes, focusing on the principles of their approaches with discussions on their features and challenges. The scope and views here are certainly limited, and many more innovative approaches and applications are expected to emerge in the coming years, for example, using semiconductor quantum dots as fluorescent probes^{101,102} and monitoring enzymatic processes in live cells.^{26–28} Moreover, the single-molecule studies of catalysis need not be limited to enzymes; catalyses of solid microcrystals by De Vos and coworkers¹⁰³ and of nanoparticles^{104–107} and carbon nanotubes¹⁰⁸ by our group are new evolving directions.

Acknowledgments

We thank Cornell University, Camille and Henry Dreyfus Foundation, National Science Foundation, Wilson Disease Association, American Chemical Society Petroleum Research Foundation, Cornell Center for Materials Research, and National Institute of Health for funding our research.

Abbreviations

FRET	fluorescence resonance energy transfer
PDMS	polydimethylsiloxane
TIR	total internal reflection

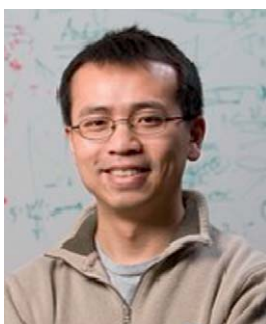
References

1. W. E. Moerner, *Proc. Natl. Acad. Sci. U.S.A.* **2007**, *104*, 12596–12602.
2. A. Ishijima; T. Yanagida, *Trends Biochem. Sci.* **2001**, *26*, 438–444.
3. J. N. Forkey; M. E. Quinlan; Y. E. Goldman, *Prog. Biophys. Mol. Biol.* **2000**, *74*, 1–35.
4. E. Toprak; P. R. Selvin, *Annu. Rev. Biophys. Biomol. Struct.* **2007**, *36*, 349–369.
5. W. J. Greenleaf; M. T. Woodside; S. M. Block, *Annu. Rev. Biophys. Biomol. Struct.* **2007**, *36*, 171–190.
6. H. Park; E. Toprak; P. R. Selvin; Q. Rev. *Biophys.* **2007**, *40*, 87–111.
7. T. Ha, *Biochemistry* **2004**, *43*, 4055–4063.
8. I. Amitani; R. J. Baskin; S. C. Kowalczykowski, *Mol. Cell* **2006**, *23*, 143–148.
9. T. T. Perkins; R. V. Dalal; P. G. Mitis; S. M. Block, *Science* **2003**, *301*, 1914–1918.
10. X. Zhuang, *Annu. Rev. Biophys. Biomol. Struct.* **2005**, *34*, 399–414.
11. J. Liphardt; B. Onoa; S. B. Smith; I. Tinoco, Jr; C. Bustamante, *Science* **2001**, *292*, 733–737.
12. D. Rueda; G. Bokinsky; M. M. Rhodes; M. J. Rust; X. Zhuang; N. G. Walter, *Proc. Natl. Acad. Sci. U.S.A.* **2004**, *101*, 10066–10071.
13. N. G. Walter, *Mol. Cell* **2007**, *28*, 923–929.
14. M. A. Ditzler; E. A. Alemán; D. Rueda; N. G. Walter, *Biopolymers* **2007**, *87*, 302–316.
15. E. Rhoades; E. Gussakovsky; G. Haran, *Proc. Natl. Acad. Sci. U.S.A.* **2003**, *100*, 3197–3202.
16. A. A. Deniz; T. A. Laurence; G. S. Belligere; M. Dahan; A. B. Martin; D. S. Chemla; P. E. Dawson; P. G. Schultz; S. Weiss, *Proc. Natl. Acad. Sci. U.S.A.* **2000**, *97*, 5179–5184.
17. E. A. Lipman; B. Schuler; O. Bakajin; W. A. Eaton, *Science* **2003**, *301*, 1233–1235.
18. B. Schuler; W. A. Eaton, *Curr. Opin. Struct. Biol.* **2008**, *18*, 16–26.
19. J. J. Benitez; A. M. Keller; P. Ochieng; L. A. Yatsunyk; D. L. Huffman; A. C. Rosenzweig; P. Chen, *J. Am. Chem. Soc.* **2008**, *130*, 2446–2447.

20. H. P. Lu; L. Y. Xun; X. S. Xie, *Science* **1998**, *282*, 1877–1882.
21. B. P. English; W. Min; A. M. van Oijen; K. T. Lee; G. Luo; Y. Sun; B. J. Cherayil; S. C. Kou; X. S. Xie, *Nat. Chem. Biol.* **2006**, *3*, 87–94.
22. L. Edman; R. Rigler, *Proc. Natl. Acad. Sci. U.S.A.* **2000**, *97*, 8266–8271.
23. K. Velonia; O. Flomenbom; D. Loos; S. Masuo; M. Cotlet; Y. Engelborghs; J. Hofkens; A. E. Rowan; J. Klafter; R. J. M. Nolte; F. C. de Schryver, *Angew. Chem. Int. Ed.* **2005**, *44*, 560–564.
24. J. R. Brender; J. Dertouzos; D. P. Ballou; V. Massey; B. A. Palfey; B. Entsch; D. G. Steel; A. Gafni, *J. Am. Chem. Soc.* **2005**, *127*, 18171–18178.
25. N. M. Antikainen; R. D. Smiley; S. J. Benkovic; G. G. Hammes, *Biochemistry* **2005**, *44*, 16835–16843.
26. J. Yu; J. Xiao; X. Ren; K. Lao; X. S. Xie, *Science* **2006**, *311*, 1600–1603.
27. L. Cai; N. Friedman; X. S. Xie, *Nature* **2006**, *440*, 358–362.
28. X. S. Xie; P. J. Choi; G.-W. Li; N. K. Lee; G. Lia, *Annu. Rev. Biophys.* **2008**, *37*, 417–444.
29. W. E. Moerner; D. P. Fromm, *Rev. Sci. Instrum.* **2003**, *74*, 3597–3619.
30. P. V. Cornish; T. Ha, *ACS Chem. Biol.* **2007**, *2*, 53–61.
31. X. Michalet; S. Weiss; M. Jaeger, *Chem. Rev.* **2006**, *106*, 1785–1813.
32. R. Roy; S. Hohng; T. Ha; *Nat. Methods* **2008**, *5*, 507–516.
33. X. Nan; P. A. Sims; P. Chen; X. S. Xie, *J. Phys. Chem. B* **2005**, *109*, 24220–24224.
34. P. R. Selvin; T. Ha; Eds, *Single Molecule Techniques: A Laboratory Manual*; Harbor Laboratory Press: Cold Spring, 2008.
35. X. S. Xie; J. K. Trautman, *Annu. Rev. Phys. Chem.* **1998**, *49*, 441–480.
36. G. Bokinsky; X. Zhuang, *Acc. Chem. Res.* **2005**, *38*, 566–573.
37. P. F. Barbara; A. J. Gesquiere; S.-J. Park; Y. J. Lee, *Acc. Chem. Res.* **2005**, *38*, 602–610.
38. T. Basche; W. E. Moerner; M. Orrit; U. P. Wild, *Single-Molecule Optical Detection, Imaging and Spectroscopy*; VCH Verlagsgesellschaft mbH: Weinheim, 1997.
39. C. Bustamante; J. C. Macosko; G. J. L. Wuite, *Nat. Rev. Mol. Cell Biol.* **2000**, *1*, 130–136.
40. A. M. van Oijen, *Biopolymers* **2007**, *85*, 144–153.
41. G. Charvin; T. R. Strick; D. Bensimon; V. Croquette, *Annu. Rev. Biophys. Biomol. Struct.* **2005**, *34*, 201–219.
42. S. A. Rosenberg; M. E. Quinlan; J. N. Forkey; Y. E. Goldman, *Acc. Chem. Res.* **2005**, *38*, 583–593.
43. P. Tinnefeld; M. Sauer, *Angew. Chem. Int. Ed.* **2005**, *44*, 2642–2671.
44. C. Dekker, *Nat. Nanotechnol.* **2007**, *2*, 209–215.
45. B. Sakmann; E. Neher; Eds., *Single-Channel Recording*; 2nd ed.; Plenum Press: New York 1995.
46. C. Joo; H. Balci; Y. Ishitsuka; C. Buranachai; T. Ha, *Annu. Rev. Biochem.* **2008**, *77*, 51–76.
47. X. S. Xie, *Single Mol.* **2001**, *2*, 229–236.
48. R. D. Smiley; G. G. Hammes, *Chem. Rev.* **2006**, *106*, 3080–3094.
49. C. R. Bagshaw; P. B. Conibear, *Single Mol.* **2000**, *4*, 271–277.
50. P. Chen; N. M. Andoy, *Inorg. Chim. Acta* **2008**, *361*, 809–819.
51. K. C. Neuman; A. Nagy, *Nat. Methods* **2008**, *5*, 491–505.
52. N. G. Walter; C. Y. Huang; A. J. Manzo; M. A. Sobhy, *Nat. Methods* **2008**, *5*, 475–489.
53. M. Vrljic; S. Nishimura; W. Moerner, *Methods Mol. Biol.* **2007**, *398*, 193–219.
54. L. Edman; Z. FiSides-Papp; S. Wennmalm; R. Rigler, *Chem. Phys.* **1999**, *247*, 11–22.
55. O. Flomenbom; K. Velonia; D. Loos; S. Masuo; M. Cotlet; Y. Engelborghs; J. Hofkens; A. E. Rowan; R. J. M. Nolte; M. van der Auweraer; F. C. de Schryver; J. Klafter, *Proc. Natl. Acad. Sci. U.S.A.* **2005**, *102*, 2368–2372.
56. M. Paige; D. P. Fromm; W. E. Moerner, *Proc. Soc. Photo-Opt. Instrum. Engr.* **2002**, *4634*, 92–103.
57. T. Ha; A. Y. Ting; J. Liang; W. B. Caldwell; A. A. Deniz; D. S. Chemla; P. G. Schultz; S. Weiss, *Proc. Natl. Acad. Sci. U.S.A.* **1999**, *96*, 893–898.
58. Y. Chen; D. Hu; E. R. Vorpapel; H. P. Lu, *J. Phys. Chem. B* **2003**, *107*, 7947–7956.
59. P. T. R. Rajagopalan; Z. Zhang; L. McCourt; M. Dwyer; S. J. Benkovic; G. G. Hammes, *Proc. Natl. Acad. Sci. U.S.A.* **2002**, *99*, 13481–13486.
60. Z. Zhang; P. T. R. Rajagopalan; T. Selzer; S. J. Benkovic; G. G. Hammes, *Proc. Natl. Acad. Sci. U.S.A.* **2004**, *101*, 2764–2769.
61. T. Funatsu; Y. Harada; M. Tokunaga; K. Saito; T. Yanagida, *Nature* **1995**, *374*, 555–559.
62. H. Engelkamp; N. S. Hatzakis; J. Hofkens; F. C. de Schryver; R. J. M. Nolte; A. E. Rowan, *Chem. Commun.* **2005**, 935–940.
63. J. Shi; J. Dertouzos; A. Gafni; D. G. Steel; B. A. Palfey, *Proc. Natl. Acad. Sci. U.S.A.* **2006**, *103*, 5775–5780.
64. J. Shi; B. A. Palfey; J. Dertouzos; K. F. Jensen; A. Gafni; D. Steel, *J. Am. Chem. Soc.* **2004**, *126*, 6914–6922.
65. G. D. Cremer; M. B. J. Roelfaers; M. Baruah; M. Sliwa; B. F. Sels; J. Hofkens; D. E. D. Vos, *J. Am. Chem. Soc.* **2007**, *129*, 15458–15459.
66. M. Comellas-Aragones; H. Engelkamp; V. I. Claessen; N. A. J. M. Sommerdijk; A. E. Rowan; P. C. M. Christianen; J. C. Maan; B. J. M. Verduin; J. J. L. M. Cornelissen; R. J. M. Nolte, *Nat. Nanotechnol.* **2007**, *2*, 635–639.
67. N. Carette; H. Engelkamp; E. Akpa; S. J. Pierre; N. R. Cameron; P. C. M. Christianen; J. C. Maan; J. C. Thies; R. Weberskirch; A. E. Rowan; R. J. M. Nolte; T. Michon; J. C. M. van Hest, *Nat. Nanotechnol.* **2007**, *2*, 226–229.
68. Q. Xue; E. S. Yeung, *Nature* **1995**, *373*, 681–683.
69. D. B. Craig; E. A. Arriaga; J. C. Y. Wong; H. Lu; N. J. Dovichi, *J. Am. Chem. Soc.* **1996**, *118*, 5245–5253.
70. Y. Rondelez; G. Tresset; K. V. Tabata; H. Arata; H. Fujita; S. Takeuchi; H. Noji, *Nat. Biotechnol.* **2005**, *23*, 361–365.
71. D. M. Rissin; H. H. Gorris; D. R. Walt, *J. Am. Chem. Soc.* **2008**, *130*, 5349–5353.
72. H. H. Gorris; D. M. Rissin; D. R. Walt, *Proc. Natl. Acad. Sci. U.S.A.* **2007**, *104*, 17680–17685.
73. A. I. Lee; J. P. Brody, *Biophys. J.* **2005**, *88*, 4303–4311.
74. T.-M. Hsin; E. S. Yeung, *Angew. Chem. Int. Ed.* **2007**, *46*, DOI: 10.1002/anie.200702348.
75. S.-Y. Jung; Y. Liu; C. P. Collier, *Langmuir* **2008**, *24*, 4439–4442.
76. M. Halim; M. S. Tremblay; S. Jockusch; N. J. Turro; D. Sames, *J. Am. Chem. Soc.* **2007**, *129*, 7704–7705.
77. J. Steffen; Q. Zheng; G. S. He; H. E. Pudavar; D. J. Yee; V. Balsanek; M. Halim; D. Sames; P. N. Prasad; N. J. Turro, *J. Phys. Chem. C* **2007**, *111*, 8872–8877.

78. D. J. Yee; V. Balsanek; D. R. Bauman; T. M. Penning; D. Sames, *Proc. Natl. Acad. Sci. U.S.A.* **2006**, *103*, 13304–13309.
79. M. K. Froemming; D. Sames, *J. Am. Chem. Soc.* **2007**, *129*, 14518–14522.
80. D. J. Yee; V. Balsanek; D. Sames, *J. Am. Chem. Soc.* **2004**, *126*, 2282–2283.
81. M. Tokunaga; K. Kitamura; K. Saito; H. A. Iwane; T. Yanagida, *Biochem. Biophys. Res. Commun.* **1997**, *235*, 47–53.
82. S. Myong; B. C. Stevens; T. Ha, *Structure* **2006**, *14*, 633–643.
83. B. W. van der Meer; G. Coker, III; S.-Y. S. Chen, *Resonance Energy Transfer: Theory and Data*; VCH Publishers, Inc.: New York, 1994.
84. R. P. Haugland, *The Handbook: A Guide to Fluorescent Probes and Labeling Technologies*; Invitrogen Corp.: California, U.S.A., 2005.
85. T. J. Ha; A. Y. Ting; J. Liang; W. B. Caldwell; A. A. Deniz; D. S. Chemla; P. G. Schultz; S. Weiss, *Proc. Natl. Acad. Sci. U.S.A.* **1999**, *96*, 893–898.
86. Z. Zhang; M. M. Spiering; M. A. Trakselis; F. T. Ishmael; J. Xi; S. J. Benkovic; G. G. Hammes, *Proc. Natl. Acad. Sci. U.S.A.* **2005**, *102*, 3254–3259.
87. J. Xi; Z. Zhuang; Z. Zhang; T. Selzer; M. M. Spiering; G. G. Hammes; S. J. Benkovic, *Biochemistry* **2005**, *44*, 2305–2318.
88. J. Xi; Z. Zhang; Z. Zhuang; J. Yang; M. M. Spiering; G. G. Hammes; S. J. Benkovic, *Biochemistry* **2005**, *44*, 7747–7756.
89. J. A. Hanson; K. Duderstadt; L. P. Watkins; S. Bhattacharyya; J. Brokaw; J.-W. Chu; H. Yang, *Proc. Natl. Acad. Sci. U.S.A.* **2007**, *104*, 18055–18060.
90. T. Ha, *Methods* **2001**, *25*, 78–86.
91. A. H. Westphal; A. Matorin; M. A. Hink; J. W. Borst; W. J. H. van Berkel; A. J. W. G. Visser, *J. Biol. Chem.* **2006**, *281*, 11074–11081.
92. S. Kuznetsova; G. Zauner; T. Aartsma; H. Engelkamp; N. Hatzakis; A. E. Rowan; R. J. M. Nolte; P. C. M. Christianen; G. W. Canters, *Proc. Natl. Acad. Sci. U.S.A.* **2008**, *105*, 3250–3255.
93. R. H. Holm; P. Kennepohl; E. I. Solomon, *Chem. Rev.* **1996**, *96*, 2239–2314.
94. B. N. G. Giepmans; S. R. Adams; M. H. Ellisman; R. Y. Tsien, *Science* **2006**, *312*, 217–224.
95. I. Rasnik; S. A. McKinney; T. Ha, *Nat. Methods* **2006**, *3*, 891–893.
96. H. Yang; G. Luo; P. Karnchanaphanurach; T.-M. Louie; I. Rech; S. Cova; L. Xun; X. S. Xie, *Science* **2003**, *302*, 262–266.
97. W. Min; G. Luo; B. J. Cherayil; S. C. Kou; X. S. Xie, *Phys. Rev. Lett.* **2005**, *94*, 198302.
98. J.-P. Knemeyer; N. Marme; M. Sauer, *Anal. Chem.* **2000**, *72*, 3717–3724.
99. O. Piester; H. Barsch; V. Buschmann; T. Heinlein; J.-P. Knemeyer; K. D. Weston; M. Sauer, *Nano Lett.* **2003**, *3*, 979–982.
100. H. B. Gray; J. R. Winkler, *Annu. Rev. Biochem.* **1996**, *65*, 537–561.
101. A. P. Alivisatos, *Science* **1996**, *271*, 933–937.
102. X. Michalet; F. F. Pinaud; L. A. Bentolila; J. M. Tsay; S. Doose; J. J. Li; G. Sundaresan; A. M. Wu; S. S. Gambhir; S. Weiss, *Science* **2005**, *307*, 538–544.
103. M. B. Roeffaers; B. F. Sels; H. Uji-i; F. C. De Schryver; P. A. Jacobss; D. E. De Vos; J. Hofkens, *Nature* **2006**, *439*, 572–575.
104. W. Xu; J. S. Kong; Y.-T. E. Yeh; P. Chen, *Nature Mater.* **2008**, *7*, 992–996.
105. W. Xu; J. S. Kong; P. Chen, *J. Phys. Chem. C* **2009**, *113*, 2393–2404.
106. W. Xu; J. S. Kong; P. Chen, *Phys. Chem. Chem. Phys.* **2009**, *11*, 2767–2778.
107. P. Chen; W. Xu; X. Zhou; D. Panda; A. Kalininskiy, *Chem. Phys. Lett.* **2009**, *470*, 151–157.
108. W. Xu; H. Shen; Y. J. Kim; X. Zhou; G. Liu; J. Park; P. Chen, *Nano Lett.* **2009**, doi:10.1021/nl900988f.

Biographical Sketches



Peng Chen received his B.S. from Nanjing University, China in 1997. After spending a year at the University of California at San Diego with Professor Yitzhak Tor, he moved to Stanford University and did his Ph.D. with Professor Edward Solomon in bioinorganic and physical inorganic chemistry. In 2004, he joined Professor Sunney Xie's group at Harvard University for postdoctoral research in single-molecule biophysics. He started his assistant professorship at Cornell University in 2005. His current research interests focus on the single-molecule imaging of bioinorganic chemistry and nanoscale catalysis. He has received a Camille and Henry Dreyfus New Faculty award, an NSF Career award, and an Alfred P. Sloan Research Fellowship.



Nesha May Andoy obtained her B.S. in chemistry at the University of the Philippines in 2001. She is currently a graduate student at Cornell University in the Department of Chemistry and Chemical Biology working in Professor Peng Chen's group. Her research covers single-molecule studies of metalloregulator–DNA interactions, bioinorganic enzymology, and nanoscale catalysis.